



Osthole-Mediated Inhibition of Neurotoxicity Induced by Ropivacaine via Amplification of the Cyclic Adenosine Monophosphate Signaling Pathway

Dose-Response:
An International Journal
January-March 2022:1-10
© The Author(s) 2022
Article reuse guidelines:
sagepub.com/journals-permissions
DOI: 10.1177/15593258221088092
journals.sagepub.com/home/dos


WeiBing Wang¹ , Hui Zhou¹, LaiBao Sun², MeiNa Li², Fengjiao Gao², Aijiao Sun³, and XueNong Zou⁴

Abstract

Background: Ropivacaine is widely used for clinical anesthesia and postoperative analgesia. However, the neurotoxicity induced by ropivacaine in a concentration- and duration-dependent manner, and it is difficult to prevent neurotoxicity. Osthole inhibits phosphodiesterase-4 activity by binding to its catalytic site to prevent cAMP hydrolysis. The aim of this present study is to explore the precise molecular mechanism of osthole-mediated inhibition of neurotoxicity induced by ropivacaine.

Methods: SH-SY5Y cell viability and apoptosis were measured in different concentration and duration. Protein concentration was determined in each signaling pathway. The molecular mechanism of osthole-mediated inhibition of ropivacaine-caused neurotoxicity was evaluated.

Results: The study demonstrated that osthole inhibits SH-SY5Y cells neurotoxicity in a duration- and concentration-dependent manner. Moreover, ropivacaine significantly increased the expression of caspase-3 by promoting the phosphorylation of p38. Osthole-induced upregulation of cAMP activated cAMP-dependent signaling pathway, sequentially leading to elevated cyclic nucleotide response element-binding protein levels, which inhibits P38-dependent signaling and decreases apoptosis of SH-SY5Y.

Conclusions: This study display the evidence confirmed the molecular mechanism by which osthole amplification of cAMP-dependent signaling pathway, and overexpression of cyclic nucleotide response element-binding protein inhibits P38-dependent signaling and decreases ropivacaine-induced SH-SY5Y apoptosis.

Keywords

ropivacaine, osthole, neurotoxicity, p38, cyclic adenosine monophosphate, apoptosis

Introduction

The local anesthetic ropivacaine is widely used for clinical anesthesia and postoperative analgesia given its reduced cardiac toxicity, and its especially useful property of inducing a separation block in sensory and motor nerves,¹⁻³ However, epidemiological investigations have shown that nerve exposure to high concentrations and long durations of local anesthetics could result in neurotoxicity.^{4,5} All local anesthetics have been reported to cause neurotoxicity in a concentration- and duration-dependent manner.⁶

¹Department of Anesthesiology, The Affiliated AnQing Municipal Hospitals of Anhui Medical University, AnQing, China

²Department of Anesthesiology, The First Affiliated Hospitals of Sun Yat-Sen University, GuangZhou, China

³Department of Cardiovascularology, The Affiliated AnQing Municipal Hospital of Anhui Medical University, AnQing, China

⁴Department of Orthopedics, The First Affiliated Hospitals of Sun Yat-Sen University, GuangZhou, China

Received 9 December 2021; accepted 30 December 2021

Corresponding Author:

Aijiao Sun, Department of Cardiovascularology, The Affiliated AnQing Municipal Hospital of Anhui Medical University, 352th, Renming Road, AnQing 246003, China.
Email: 1011356643@qq.com



Creative Commons Non Commercial CC BY-NC: This article is distributed under the terms of the Creative Commons Attribution-NonCommercial 4.0 License (<https://creativecommons.org/licenses/by-nc/4.0/>) which permits non-commercial use, reproduction and distribution of the work without further permission provided the original work is attributed as specified on the SAGE

and Open Access pages (<https://us.sagepub.com/en-us/nam/open-access-at-sage>).

The precise molecular mechanism of neurotoxicity induced by ropivacaine is unclear, inflammation, neurotrophic factors, cell apoptosis, and intracellular calcium concentration are generally related to neurotoxicity.⁷⁻¹⁰

Ropivacaine, introduced as a pure S-(–)-enantiomer, has a low degree of neurotoxicity, but high concentration of ropivacaine triggers both neurotoxicity and cardiovascular toxicity. Several previous studies indicate that neurotoxicity induced by ropivacaine including mitochondrial dynamics, mitochondrial dysfunction and cell death that are dependent on dynamic reaction protein 1 (DRP1) expression,¹¹ and CaMKII β , Cav3.2, Cav3.3 expression up-regulated.^{12,13} Ropivacaine inhibits the tuberlin/mTOR/p70S6K signaling pathway, downregulates autophagic flux, and increases neuronal damage.¹⁴ Researchers have suggested that ropivacaine activates the MAPK/p38/Fas signaling pathway to promote neurogliaocyte apoptosis,¹⁵ but a consensus on the molecular mechanism of neurotoxicity induced by ropivacaine is lacking.

Phosphodiesterase-4 (PDE4) reduces intracellular cyclic adenosine monophosphate (cAMP) levels by hydrolyzing cAMP to 5'-AMP, thereby regulating the cAMP/PKA pathway and the phosphorylation of cyclic nucleotide response element-binding protein (CREB) by PKA.^{16,17} PDE4-selective inhibitors interact with the catalytic pocket of the enzyme and decrease cAMP hydrolysis, as a result, the cAMP levels were increased intracellularly. The major effect of higher cAMP levels is the activation of the cAMP-dependent cAMP/PKA/CREB pathway. Greater than 20 naturally occurring PDE4 isoforms, are encoded by 4 genes (PDE4A, PDE4B, PDE4C, and PDE4D), each of which has a specific pattern of expression.¹⁸ PDE4D5 could determine the direction of the pathway by regulating the levels of several signaling proteins, such as RACK1,¹⁹ β -arrestin2,²⁰⁻²² and the MAPK signaling pathway, especially ERK1/2²³⁻²⁵ and MK2.²⁶ PDE4D5 is also a PKA²⁷ and oxidative-stress kinase target.²⁸

Osthole is a coumarin derivative (She Chuang Zi) that is, a widely used traditional Chinese medicine, and has many biological functions.²⁹ Osthole displays anti-inflammatory biological functions by suppressing the activation of the NF- κ B and p38/MAPK signaling pathways,³⁰ and anti-gastric cancer activity inhibition the AKT/MAPK pathway.³¹ Osthole is also effective in preventing the colitis by suppressing p38/MAPK and cAMP/PKA-dependent pathways,³² and osthole modifies osteogenesis by activating the cAMP/PKA/CREB signaling pathway.³³ Recently, a study demonstrated that osthole inhibited PDE4D activity by binding to the PDE4D catalytic site to prevent cAMP hydrolysis, therefore, the cAMP levels were increased and amplified cAMP/PKA-dependent signaling, eventually resulting in relaxation of airways in airway smooth muscle cells.³⁴ Despite studies addressing several biochemical behaviors of osthole, whether osthole exerts the property for the inhibition of neurotoxicity induced by ropivacaine and its molecular mechanisms remain elusive.

In the present study, we found that SH-SY5Y cell neurotoxicity was induced by ropivacaine in a concentration- and

duration-dependent manner, and that osthole inhibited neurotoxicity induced by ropivacaine in a concentration- and duration-dependent manner. Osthole inhibits PDE4D activity and decreases the hydrolysis of cAMP to 5'-AMP, thereby increasing cAMP levels and activating the cAMP/PKA/CREB pathway, CREB over expression suppresses p38/MAPK pathways and decreases SH-SY5Y cell apoptosis.

Materials and Methods

Reagents and Cells

SH-SY5Y cells with special culture medium, bovine serum albumin and all of the antibodies were purchased from Jihe Biotechnology Inc, Shanghai. The TUNEL apoptosis assay kit and total RNA extraction kit were purchased from Jingchu Biotechnology Co.,Ltd, Shanghai. Masson kit and streptavidin were purchased from Jingheng Biotechnology Co.,Ltd, Shanghai. Osthole with a purity greater than 98% was purchased from Mansite Biotechnology Inc, Chengdu. Ropivacaine at a concentration of 1% was purchased from AstraZeneca AB Ltd

Viability Assays for SH-SY5Y Cells

SH-SY5Y cells were cultured with 10% complete medium (minimum essential medium, MEM, supplemented with 10% FBS, L-glutamine (2 mM), penicillin (50 U/ml), streptomycin (50 mg/ml)) in a humidified, 5% CO₂, 37°C incubator. The medium was replaced every 2 days, and then the cells were passages when they reached to 90% confluence.

The passaging cells were plated at 2×10^5 cells/ml in 6-well plates and 2 mL/well at 37°C with 5% CO₂ for 24h, and then stimulated with six different concentration of ropivacaine, .1, .5, 1.0, 2.0, 5.0, and 10.0 mM for 8 h. Then, cells were sequentially cultured at 37°C with 5% CO₂ for 7 days. Cell viability was measured using a trypan blue exclusion assay. The growth medium was replaced every 2 days, and images of SH-SY5Y cells were captured every day with an inverted microscope (Olympus, Tokyo, Japan). Following imaging, SH-SY5Y cells were trypsinized and stained with trypan blue (Mediatech, Manassas, VA, USA). A hemocytometer (Beckman, Brea, CA, USA) was used to count viable (nonstained) and nonviable (blue) cells.

Neurotoxicity Assay to Assess Osthole's Preventative Effects

Osthole was diluted into dimethyl sulfoxide (DMSO) and mixed with culture medium to supply six different concentrations. SH-SY5Y cells were pre-treated with different concentrations of osthole for 1 h, before subsequent treatment of ropivacaine (3 mM) for 8 h, and then cells were cultured in growth medium for 7 days. Cell viability was measured using a trypan blue exclusion assay.

Flow Cytometry to Assess SH-SY5Y Cell Apoptosis

SH-SY5Y cells were cultured at 2×10^5 cells/ml in 6-well plates and 2 mL/well at 37°C with 5% CO₂ for 24 h. Cells were stimulated with normal saline for 8 h and then culture with growth medium for 28d in control group, or cells were stimulated with 3.0 mM ropivacaine for 8 h and then culture with growth medium for 28d in ropivacaine group. Cells were pre-treated with 100 μM osthole for 1 h, before subsequent treatment of ropivacaine (3.0 mM) for 8 h, and then cells were cultured in growth medium for 28 days in osthole group. After 28 days, the rate of apoptosis was measured. (Figure 1.)

After 28 d of culture, cells were digested by adding .5 mL of trypsin to each well and then centrifuged at 1500 r/min for 5 min. The supernatant was discarded, and cells were washed with 1 mL of cold PBS in each group. Cells were centrifuged at 1500 r/min for 5 min, discarding the supernatant. Then, 300 μL Binding Buffer and 5 μL Annexin V-FITC were added in each group and incubated in the dark for 15 min. Cells were resuspended in 200 μL Binding Buffer, 5 min prior to analysis using a BD FACSCalibur flow cytometry. Then 10 μL PI was added in each group. A minimum of 1.0×10^4 cells within the gated region were analyzed.

Western Blotting

SH-SY5Y cell samples were lysed for 20 min placed on ice in RIPA lysis buffer and centrifuged at 12 000 r/min for 20 min at 4°C, and the supernatant was reserved.

Protein concentration was determined using a bicinchoninic acid (BCA) protein concentration assay kit. The protein concentration was adjusted by adding 5×loading buffer and PBS according to the concentration determination results to ensure a consistent protein concentration between different groups. After the concentration was adjusted, the samples were incubated at 95°C for 5 min.

Protein samples were electrophoretically separated using a 10% SDS polyacrylamide gel, followed by transfer to .45 μm

PVDF membranes at 200 mA for 90 min. PVDF membranes were soaked in TBST (containing 5% skim milk) for 2 h at room temperature, and the PVDF membrane was subsequently soaked in primary antibody (1:1000) diluted with TBST (containing 2% BSA solution) and incubated at 4°C overnight. After washing with TBST thrice, the HRP labeled secondary antibody was diluted (1:1500) with TBST, and the PVDF membrane was soaked in the secondary antibody solution for 1 h at room temperature.

The results were visualized using an automatic chemiluminescence image analysis system (Beyotime Biotechnology Co.,Ltd, Shanghai, China). Image grayscale values were analyzed using Image J software.

Assay to Determine PDE Activity in Vitro

The PDELight HTS cAMP phosphodiesterase kit (Lonza, LT07-600) was used to determine PDE activity, per operated according to the manufacturer's instructions (Protocol B). One microliter of PDE eluate expressed in eukaryotes was incubated with osthole for 20 min in PDE buffer (10 mM Tris-HCl, pH = 7.5). Then, 2 μM of cAMP was added, and the solution was kept under incubation for 60 minutes. Then, 10 μl of the stop solution was added to the reaction to stop further phosphodiesterase activity, and 20 μl of the reconstituted AMP detection reagent was then added to the wells followed by incubate for 10 minutes at room temperature, luminescence was measured using a Varioskan Flash device (Thermo Fisher Scientific) after 10 minutes later.

Statistical Analysis

SPSS 17.0 (SPSS Inc., Chicago, IL, USA) was used for all statistics. Parametric data expressed as mean ± standard deviation (mean ± SD), One-way analysis of variance (one-way ANOVA) was used for comparisons between groups. Kruskal-Wallis test was conducted for analysis of normalized data. A *P*-value less than .05 was considered statistically significant.

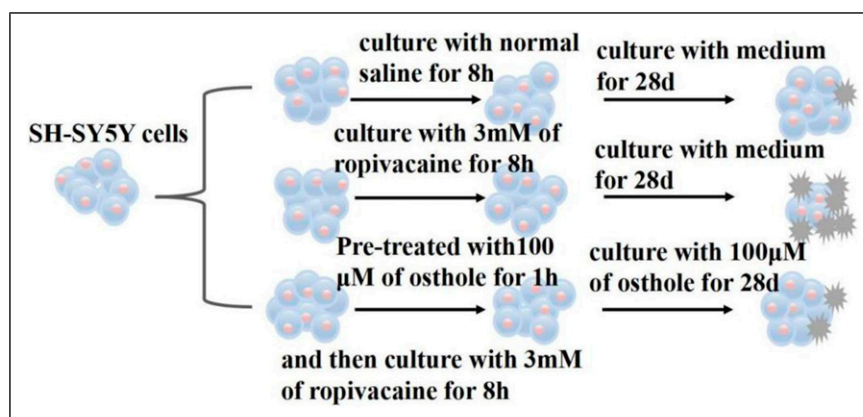


Figure 1. The different stimulation methods of SH-SY5Y cells in three groups.

Results

The IC_{50} of ropivacaine inhibits SH-SY5Y cells viability.

SH-SY5Y cells were stimulated with six different concentrations (.1, .5, 1.0, 2.0, 5.0, and 10.0 mM) of ropivacaine for 8 h, then the cells were sequentially cultured in growth medium. We counted the percentage of death cells in each concentration (8%, 12%, 48%, 69%, 73%, 80%, respectively) after 72 h, and calculated the mean inhibitory concentration (IC_{50}) by probit regression analysis from twelve experiments. The IC_{50} of ropivacaine that inhibited SH-SY5Y cells viability was 3.22 ± 1.1 mM (Figure 2A). Ropivacaine significantly inhibited SH-SY5Y cells viability compared with the control. The neurotoxicity caused by ropivacaine was duration- and concentration-dependent (Figure 2B).

The IC_{50} of osthole-mediated inhibition of SH-SY5Y cell neurotoxicity

The IC_{50} of osthole-mediated inhibition of SH-SY5Y cell neurotoxicity induced by ropivacaine was 28.6 ± 6.2 μ M and the IC_{80} was 95.0 ± 12.6 μ M (Figure 3A). SH-SY5Y viability was significantly lower in the ropivacaine group compared with the control group, and the SH-SY5Y viability was no significantly different between the osthole group and the control group (Figure 3B). Osthole exerted its effects in a duration- and concentration-dependent manner to prevent neurotoxicity induced by ropivacaine.

Osthole attenuated SH-SY5Y cells apoptosis rate induced by ropivacaine

Flow cytometry results showed that the SH-SY5Y cells apoptosis rate was significantly decreased in the osthole group compared with the control and ropivacaine groups, and ropivacaine significantly increased the rate of apoptosis (Figures 4A-4D).

The cAMP/PKA and p38/MAPK signaling pathway were involved in the effects of osthole.

The protein level of cAMP was significantly increased in osthole group compared with ropivacaine group (Figure 5A), the expression of p-PKA and p-CREB were increased in osthole group compared with ropivacaine group (Figure 5B and 5C). However, the protein level of p-p38 and Caspase-3 were decreased in osthole group compared with ropivacaine group (Figure 5D and 5E).

Osthole Inhibits PDE4D5 Activity in Vitro

Osthole inhibited the activity of PDE4D5 in a concentration-dependent manner, and the IC_{50} of osthole inhibition of PDE4D5 activity was 6.22 ± 2.6 μ M. (Figure 6).

The molecular mechanism of osthole inhibition of neurotoxicity induced by ropivacaine

Local anesthetics-mediated including ropivacaine inhibition of G α s protein-coupled receptor, which decreased the activity of adenylate cyclase (AC) and decreased the cAMP levels. Osthole inhibits PDE4D activity, which decreased the hydrolysis of cAMP, therefore, the cAMP levels were increased and amplified the cAMP/PKA signaling pathway, sequentially leading to elevated CREB levels, CREB overexpression inhibits p-P38/MAPK signaling and decreases apoptosis of SH-SY5Y cells induced by ropivacaine. (Figure. 7)

Discussion

The present study demonstrated that osthole inhibits the activity of PDE4D and amplified the cAMP/PKA-dependent signaling pathway in SH-SY5Y cells, which suppresses the

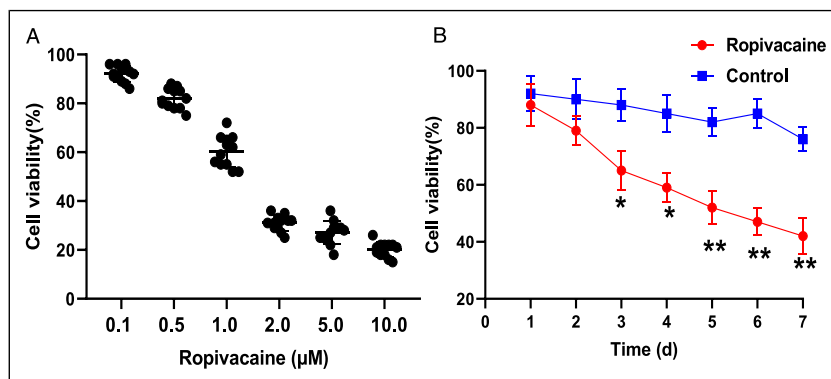


Figure 2. Concentration- and time-dependent SH-SY5Y cell neurotoxicity induced by ropivacaine. (A) SH-SY5Y cells were stimulated with six different concentrations of ropivacaine for 8 h, and the cells were sequentially cultured in growth medium. Cells viability was measured after 72 h. The IC_{50} of ropivacaine-induced SH-SY5Y cell neurotoxicity was calculated by probit regression analysis using the results from twelve experiments with six different concentrations of ropivacaine, and the IC_{50} was 3.22 ± 1.1 mM. (B) SH-SY5Y cells stimulated with 3.0 mM of ropivacaine or normal saline (control) for 8 h, and the cells were sequentially cultured in growth medium for 7 days. SH-SY5Y cell viability was significantly lower in the ropivacaine group compared with the control group (n = 3). Data are presented as the means \pm SD, and were analyzed using Kruskal–Wallis test, *P < .01, **P < .001.

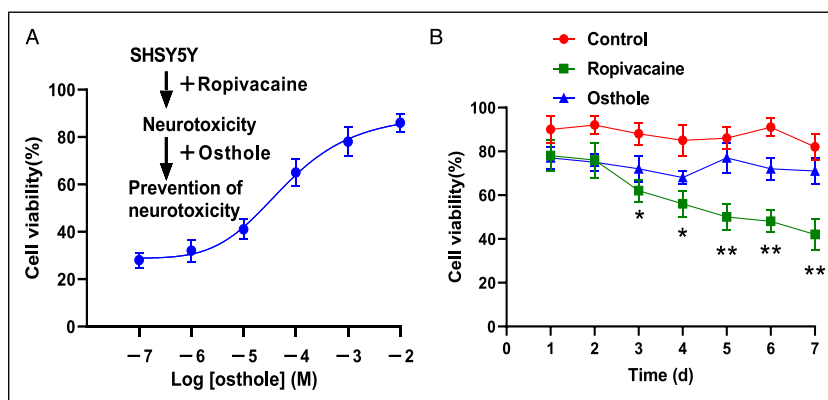


Figure 3. Concentration- and duration-dependent osthole inhibits SH-SY5Y cell neurotoxicity induced by ropivacaine. (A) Sigmoid-shaped curves for the concentration-response relationship were calculated by probit regression analysis using the results from twelve experiments with six different concentrations of osthole. The IC_{50} of osthole-mediated inhibition of SH-SY5Y cell neurotoxicity induced by ropivacaine was $28.6 \pm 6.2 \mu\text{M}$ and the IC_{90} was $95.0 \pm 12.6 \mu\text{M}$. (B) SH-SY5Y cells were stimulated with 3.0 mM of ropivacaine (ropivacaine group) or normal saline (control) for 8 h. The cells were sequentially cultured with 100 μM (osthole) or normal saline (control and ropivacaine group) for 7 days. SH-SY5Y cell viability was significantly lower in the ropivacaine group compared with the control group, and SH-SY5Y cell viability was not significantly different between the osthole group and the control group ($n = 3$). Data are represented as the means \pm SD, and were analyzed using Kruskal–Wallis test, * $P < .01$, ** $P < .001$.

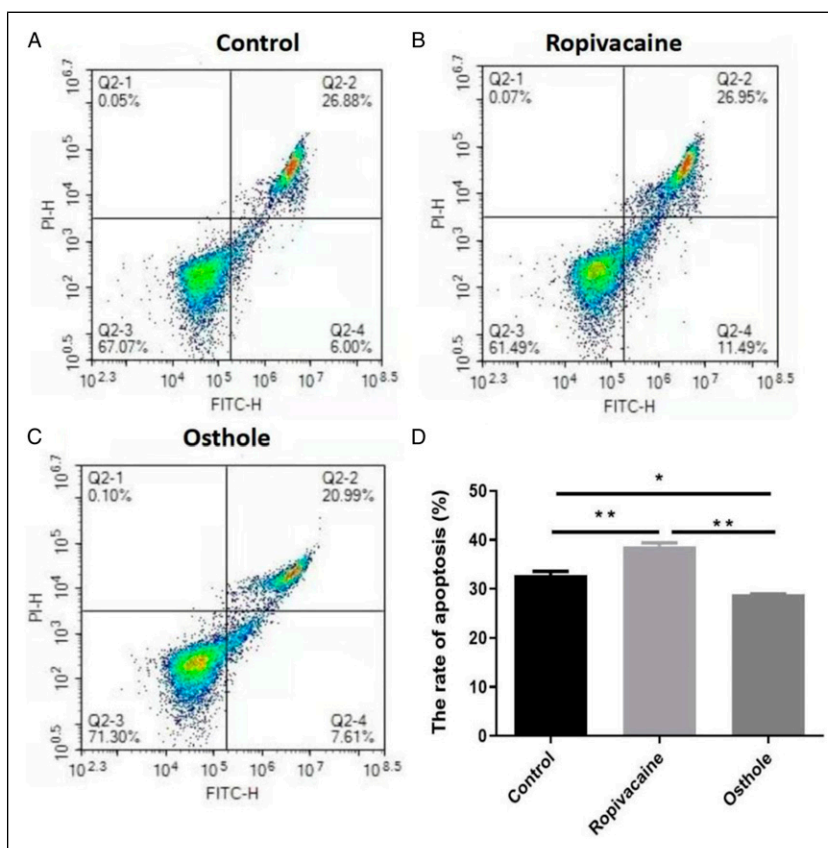


Figure 4. Osthole inhibits SH-SY5Y cell apoptosis induced by ropivacaine. (A), (B), and (C) show the rate of apoptosis in the three groups. (D) The rate of apoptosis in the ropivacaine group ($38.4 \pm 1.6\%$) was significantly increased compared with the control ($32.88 \pm 1.5\%$), and the osthole group ($28.6 \pm 1.0\%$). Apoptosis was determined by flow cytometry. All data are reported as the means \pm SD, and were analyzed using Kruskal–Wallis test, ($n = 4$), * $P < .05$ and ** $P < .01$.

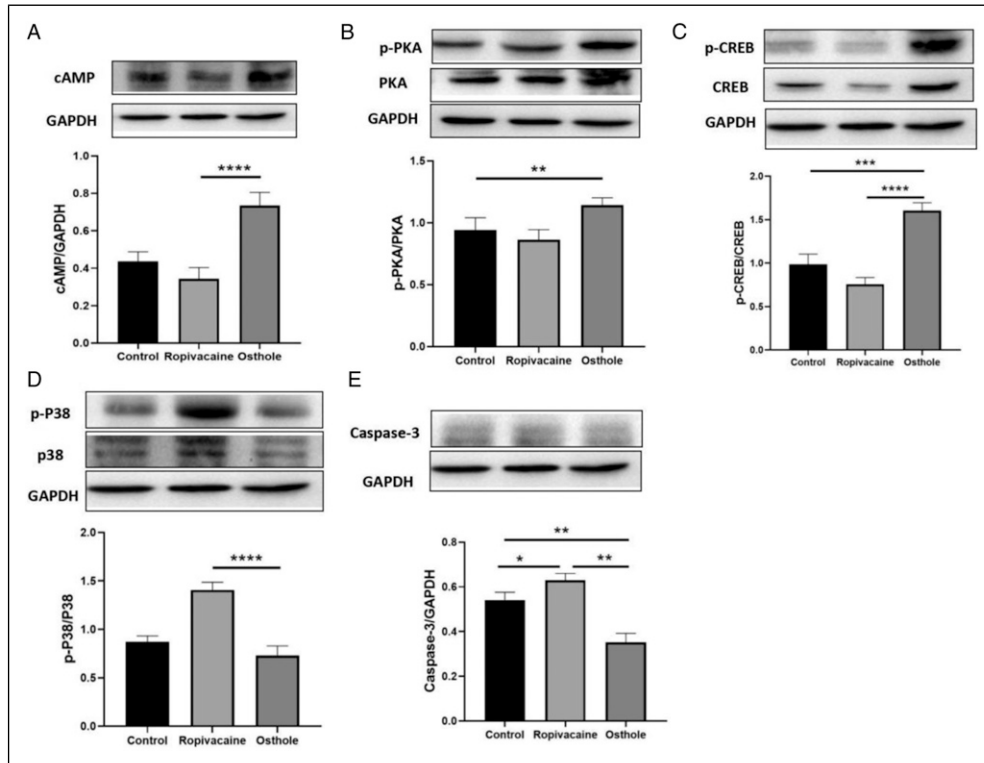


Figure 5. Osthole augments cAMP-mediated signaling and inhibits p38/MAPK signaling in SH-SY5Y cells. (A)–(C) The expression of cAMP, p-PKA, PKA, p-CREB, and CREB in the osthole group was increased compared with that in the control group, (D)–(E) The expression of p-38, p38, and caspase-3 in the osthole group was decreased compared with that in the control group. All data are presented as the means \pm SD ($n = 3$), and were analyzed using Kruskal–Wallis test, * $P < .05$ and ** $P < .01$, *** $P < .001$, **** $P < .0001$. GAPDH, glyceraldehyde-3-phosphate dehydrogenase.

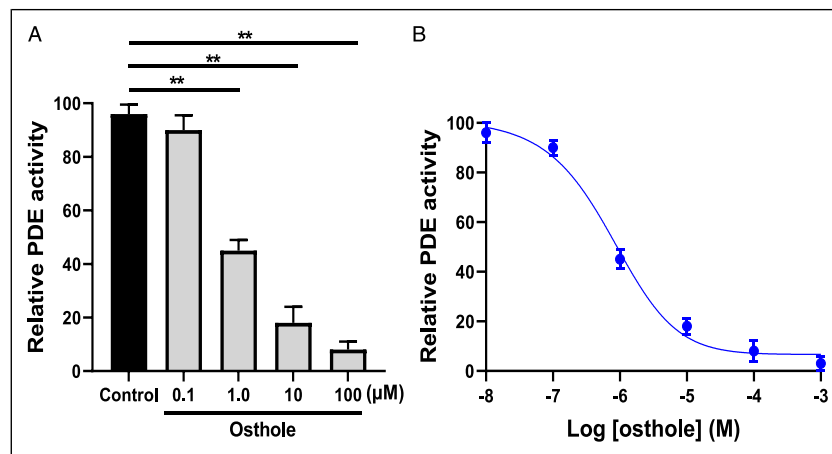


Figure 6. Osthole inhibits the activity of PDE4D5. (A) Osthole inhibited the activity of PDE in a concentration-dependent manner, and 1.0 μ M osthole efficiently inhibited the activity of PDE4D5 compared with the control group ($n = 3$). (B) Concentration-response curve of osthole inhibition of PDE4D5 activities. Sigmoid-shaped curves for the concentration-response relationship were calculated by probit regression analysis using the results from twelve experiments with six different concentrations of osthole. The IC₅₀ of osthole inhibition of PDE4D5 activity was $6.22 \pm 2.6 \mu\text{M}$. All data are presented as the means \pm SD, and were analyzed using Kruskal–Wallis test, ** $P < .01$.

p-38/MAPK-dependent signaling pathway and decreases SH-SY5Y cell apoptosis induced by ropivacaine. A previous study showed that osthole binding of catalytic sites on PDE4D5 inhibits PDE activity.³⁴

SH-SY5Y cell damage induced by ropivacaine in a concentration- and time-dependent manner,¹¹ and the study showed that SH-SY5Y cells were exposed to different concentrations of ropivacaine for 20 minutes. Cell death was induced by

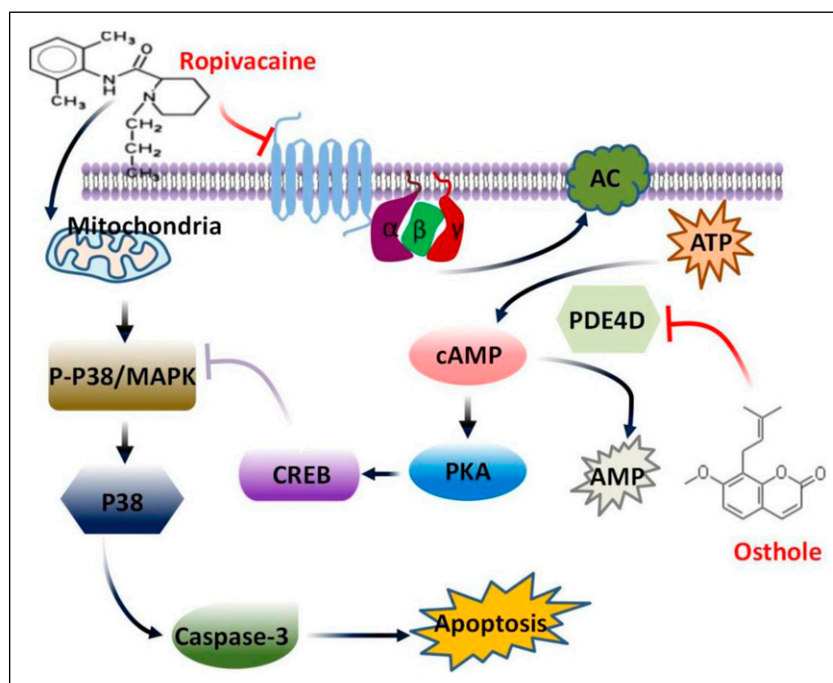


Figure 7. A proposed molecular mechanism of osthole inhibition of neurotoxicity induced by ropivacaine. Ropivacaine inhibits *G*_s-coupled receptors and decreases the cAMP levels. Osthole inhibits PDE4D activity to increase cAMP levels and amplify the cAMP/PKA signaling pathway, sequentially leading to elevated CREB levels, CREB overexpression inhibits p-P38/MAPK signaling and decreases apoptosis of SH-SY5Y cells induced by ropivacaine.

ropivacaine in a concentration-dependent manner, and the 50% cell lethality (IC₅₀) of ropivacaine was $13.43 \pm .61$ mM.³⁵ This higher concentration of ropivacaine is unsuitable for long duration clinical anesthesia. In our study, we used SH-SY5Y cells stimulated with different concentrations of ropivacaine for 8 h, the cells viability was inhibited by ropivacaine in a concentration-dependent manner. The IC₅₀ of ropivacaine-induced SH-SY5Y neurotoxicity was 3.22 ± 1.1 mM, (Figure 2A). Then, SH-SY5Y cells were stimulated with 3.0 mM of ropivacaine for 8 h, and cell viability was inhibited by ropivacaine in a time-dependent manner, (Figure 2B) SH-SY5Y cell viability was significantly inhibited in the ropivacaine group compared with the control group.

Some previous results demonstrated that osthole inhibited cell neurotoxicity in a concentration- and time-dependent manner.^{33,34} Our results confirmed that osthole prevented SH-SY5Y neurotoxicity induced by ropivacaine in the same manner. The IC₅₀ of osthole inhibited SH-SY5Y cell neurotoxicity induced by ropivacaine was 28.6 ± 6.2 μM and the IC₈₀ was 95.0 ± 12.6 μM (Figure 3A), and then we used 100 μM of osthole to prevent the SH-SY5Y neurotoxicity in a time-dependent manner. SH-SY5Y viability was significantly higher in the osthole group compared with that in the ropivacaine group (Figure 3B).

The cAMP levels determined the cAMP signaling output response by increasing cAMP synthesis or hydrolysis, and the PDE-mediated cAMP signaling output was amplified when

the cAMP levels increased.³⁶ Ropivacaine inhibits *G*_s-coupled receptors in a stereoselective and noncompetitive manner, which decrease the cAMP levels.³⁷ However, osthole inhibits PDE4D activity by binding to the PDE4D catalytic site,³⁴ and increases the cAMP levels, the present data suggest that osthole significantly inhibits PDE4D activity (Figure 6A), and in a concentration-dependent manner (Figure 6B).

Caspase-3 is an important indicator of apoptosis when assessing the neurotoxicity of various therapies. Caspase-3 is responsible for cell apoptosis in vivo, and down regulating the expression of caspase-3 decreases the rate of apoptosis.³⁸ SH-SY5Y cells were divided into three groups, and cultured with different methods, respectively (Figure 1). Our results indicated that caspase-3 protein expression levels were down-regulated in the osthole-treated group, and the rate of apoptosis was significantly decreased in the osthole group compared with the control and ropivacaine groups (Figures 4A-4D). Furthermore, we investigated the cAMP/PKA signaling pathway. The protein expression levels were increased in the osthole-treated group, and a higher level of CREB suppressed the phosphorylation level of p-38, which decreased the rate of apoptosis cells induced by ropivacaine in SH-SY5Y cells.

The clinical concentration of ropivacaine can cause neurotoxicity, however, the molecular mechanism remains unclear. In our present study, both the cAMP/PKA and p-38/MAPK signaling pathways were investigated in

osthole-treated SH-SY5Y cells. PKA is a major downstream target of cAMP. The cAMP/PKA signaling pathway plays important roles in regulating CREB by increasing P-CREB phosphorylation levels. This study showed that the molecular mechanism of neurotoxicity induced by ropivacaine involved the p-38/MAPK-dependent signaling pathway activated by ropivacaine and resulted in the promotion of neuroglial cell apoptosis.¹³ Our western blot results showed that osthole augmented cAMP/PKA signaling and elevated cAMP, PKA, and CREB protein expression (Figures 5A-5C). CREB overexpression suppressed the p38/MAPK-dependent signaling pathway, and p38 and caspase-3 protein expression decreased (Figures 5D-5E). Therefore, SH-SY5Y cell apoptosis was decreased. The study also demonstrated that cynomorium songaricum Rupr (a traditional Chinese medicine) exhibited potential therapeutic effect on neuroprotection of ovariectomized rats, and its effect was possibly exerted by p-CREB/BDNF mediated down regulation of ERK/p38MAPK.³⁹

Together, these results demonstrated that osthole-mediated prevention of SH-SY5Y cell neurotoxicity induced by ropivacaine augments the cAMP/PKA signaling output response to suppress p38/MAPK signaling and decrease SH-SY5Y cell apoptosis (Figure 7). Osthole binds to the PDE4D catalytic site and inhibits PDE4D activity, which decreases PDE4D-mediated hydrolysis of cAMP to 5'-AMP and increases cAMP levels to augment the cAMP/PKA/CREB pathway. Therefore, CREB overexpression suppressed p38/MAPK pathways and decreased SH-SY5Y cell apoptosis.

There are several limitations in this study, PDE4D-specific inhibitors should be applied to investigate the activity of PDE4Ds given that osthole, is not a specific inhibitor. The augmented cAMP/PKA signaling pathway elevated the expression of CREB, and the mechanism by which CREB suppressed the p38/MAPK-dependent signaling pathway to be demonstrated in future studies. However, the present results support the study of this promising signaling pathway in animal models in the future. Despite these limitations, osthole-induced augmentation of the cAMP/PKA signaling response upregulation of p-CREB, and suppression of p38/MAPK signaling. Thus, osthole may represent a novel therapeutic target for the inhibition of neurotoxicity induced by ropivacaine.

Conclusions

In summary, the present study demonstrated that osthole prevented neurotoxicity induced by ropivacaine by augmenting cAMP/PKA signaling output to suppress p38/MAPK signaling and decreasing apoptosis induced by ropivacaine. Osthole inhibits PDE4D activity and increases cAMP levels to promote the cAMP/PKA/CREB pathway, p38/MAPK signaling was suppressed by elevated CREB levels, and decreased SH-SY5Y cell apoptosis was noted. This study provides novel biological

evidence for osthole inhibition of neurotoxicity induced by ropivacaine.

Acknowledgments

The authors would like to thank all staff members in the Department of anesthesia, AnQing Municipal Hospitals of Anhui Medical University. The authors sincerely thank AiJiaoSun, M.D for his contributions to the whole trial design and his assistance with the study. The authors acknowledge Miss. Hui Zhou, who performed data extraction, and Miss. MeiNa Li and FengJiao Gao, who helped review the study design and data analysis. The authors are particularly grateful to Professor Pan Tao's guidance.

Declaration of Conflicting Interests

The author(s) declared no potential conflicts of interest with respect to the research, authorship, and/or publication of this article.

Funding

The author(s) disclosed receipt of the following financial support for the research, authorship, and/or publication of this article: The authors would like to thank for PhD Start-up Fund of AnQing Municipal Hospitals of Anhui Medical University, and the Nature Fund of Anqing science and Technology Bureau (NO:2020Z4003).

ORCID iD

WeiBing Wang  <https://orcid.org/0000-0002-6059-7916>

References

1. Xuebi T, Ping Y, Tiefen S, et al. Intraperitoneal ropivacaine and early postoperative pain and postsurgical outcomes after laparoscopic herniorrhaphy in toddlers: a randomized clinical trial. *Pediatric Anesthesia*. 2016;26(9):891-898.
2. Božidar B, Miroslav A, Dejan Č, et al. Efficacy and safety of 1% ropivacaine for postoperative analgesia after lower third molar surgery: a prospective, randomized, double-blinded clinical study. *Clin Oral Invest*. 2017;21(3):779-785.
3. Li M, Wan L, Mei W, Tian Y. Update on the clinical utility and practical use of ropivacaine in Chinese patients. *Drug Design, Development and Therapy*. 2014;8(9):1269-1276.
4. El-Boghdady K, Chin KJ. Local anesthetic systemic toxicity: Continuing professional development. *Canadian Journal of Anesthesia/Journal canadien d'anesthésie*. 2016; 63(3):330-349.
5. Farber SJ, Saheb-Al-Zamani M, Zieske L, Laurido-Soto O, Bery A, Hunter D, et al. Peripheral nerve injury after local anesthetic injection. *Anesth Analg*. 2013;117(3):731-739.
6. Werdehausen R, Fazeli S, Braun S, Hermanns H, Essmann F, Hollmann MW, et al. Apoptosis induction by different local anaesthetics in a neuroblastoma cell line. *Br J Anaesth*. 2009; 103(5):711-718.
7. Radwan IAM, Saito S, Goto F. The neurotoxicity of local anesthetics on growing neurons: a comparative study of lidocaine,

- bupivacaine, mepivacaine, and ropivacaine. *Anesth Analg*. 2002; 94(2):319-324.
8. Kitagawa N, Oda M, Totoki T. Possible mechanism of irreversible nerve injury caused by local anesthetics. *Anesthesiology*. 2004;100(4):962-967.
 9. Radwan IAM, Saito S, Goto aF. Neurotrophic factors can partially reverse morphological changes induced by mepivacaine and bupivacaine in developing sensory neurons. *Anesth Analg*. 2003;97(2):506-511.
 10. Kasaba T, Onizuka S, Kashiwada M, Takasaki M. Increase in intracellular Ca²⁺ concentration is not the only cause of lidocaine-induced cell damage in the cultured neurons of *Lymnaea stagnalis*. *J Anesth*. 2006;20(3):196-201.
 11. Chen Y, Yan L, Zhang Y, Yang X. The role of DRP1 in ropivacaine-induced mitochondrial dysfunction and neurotoxicity. *Artificial Cells, Nanomedicine, and Biotechnology*. 2019; 47(1):1788-1796.
 12. Wen X, Li Y, Liu X, Sun C, Lin J, Zhang W, et al. Roles of CaMKII β in the neurotoxicity induced by ropivacaine hydrochloride in dorsal root ganglion. *Artificial Cells, Nanomedicine, and Biotechnology*. 2019;47(1):2948-2956.
 13. Wen X, Liang H, Li H, Ou W, Wang HB, Liu H, et al. In vitro neurotoxicity by ropivacaine is reduced by silencing Cav3.3 T-type calcium subunits in neonatal rat sensory neurons. *Artificial cells, nanomedicine, and biotechnology*. 2018;46(8):1617-1624.
 14. Jingwei X, Qiuyue K, Leyang D, et al. Autophagy activated by tuberin/mTOR/p70S6K suppression is a protective mechanism against local anaesthetics neurotoxicity. *J Cell Mol Med*. 2017; 21(3):579-587.
 15. Shuai W, Quan L, Zhengjie W, Pan X. Ropivacaine induces neurotoxicity by activating MAPK/p38 signal to upregulate Fas expression in neurogliaocyte. *Neurosci Lett* 2019;27706(7):7-11.
 16. Guo H, Cheng Y, Wang C, Wu J, Zou Z, Niu B, et al. FPPM, a PDE4 inhibitor, reverses learning and memory deficits in APP/PS1 transgenic mice via cAMP/PKA/CREB signaling and anti-inflammatory effects. *Neuropharmacology*. 2017;116(4): 260-269.
 17. Li H, Li J, Zhang X, Feng C, Fan C, Yang X, et al. DC591017, a phosphodiesterase-4 (PDE4) inhibitor with robust anti-inflammation through regulating PKA-CREB signaling. *Biochem Pharmacol*. 2020;177(7):113958.
 18. Johnson KR, Nicodemus-Johnson J, Danziger RS. An evolutionary analysis of cAMP-specific Phosphodiesterase 4 alternative splicing. *BMC Evolutionary Biology*. 2010;1110(8):247.
 19. Bolger GB. RACK1 and β -arrestin2 attenuate dimerization of PDE4 cAMP phosphodiesterase PDE4D5. *Cell Signal*. 2016; 28(7):706-712.
 20. Richter W, Day P, Agrawal R, Bruss MD, Granier S, Wang YL, et al. Signaling from β 1- and β 2-adrenergic receptors is defined by differential interactions with PDE4. *EMBO J*. 2008;27(2): 384-393.
 21. Bradaia A, Berton F, Ferrari S, Lüscher C. β -Arrestin2, interacting with phosphodiesterase 4, regulates synaptic release probability and presynaptic inhibition by opioids. *Proc Natl Acad Sci Unit States Am*. 2005;102(8):3034-3039.
 22. Li X, Huston E, Lynch MJ, Houslay MD, Baillie GS. Phosphodiesterase-4 influences the PKA phosphorylation status and membrane translocation of G-protein receptor kinase 2 (GRK2) in HEK-293beta2 cells and cardiac myocytes. *Biochem J*. 2006; 394(Pt 2):427-435.
 23. Hoffmann R, Baillie GS, MacKenzie SJ, Yarwood SJ, Houslay MD. The MAP kinase ERK2 inhibits the cyclic AMP-specific phosphodiesterase HSPDE4D3 by phosphorylating it at Ser579. *EMBO J*. 1999;18(4):893-903.
 24. MacKenzie SJ, Baillie GS, McPhee I, Bolger GB, Houslay MD. ERK2 Mitogen-activated Protein Kinase Binding, Phosphorylation, and Regulation of the PDE4D cAMP-specific Phosphodiesterases. *J Biol Chem*. 2000;275(22):16609-16617.
 25. Song RS, Massenburg B, Wenderski W, Jayaraman V, Thompson L, Neves SR. ERK regulation of phosphodiesterase 4 enhances dopamine-stimulated AMPA receptor membrane insertion. *Proc Natl Acad Sci Unit States Am*. 2013;110(38):15437-15442.
 26. Houslay KF, Christian F, MacLeod R, Adams DR, Houslay MD, Baillie GS. Identification of a multifunctional docking site on the catalytic unit of phosphodiesterase-4 (PDE4) that is utilised by multiple interaction partners. *Biochem J*. 2017;474(4):597-609.
 27. Sette C, Conti M. Phosphorylation and Activation of a cAMP-specific Phosphodiesterase by the cAMP-dependent Protein Kinase. *J Biol Chem*. 1996;271(28):16526-16534.
 28. Hill EV, Sheppard CL, Cheung Y-F, Gall I, Krause E, Houslay MD. Oxidative stress employs phosphatidylinositol 3-kinase and ERK signalling pathways to activate cAMP phosphodiesterase-4D3 (PDE4D3) through multi-site phosphorylation at Ser239 and Ser579. *Cell Signal*. 2006;18(11): 2056-2069.
 29. Zhang ZR, Leung WN, CheungCheung HY, Chan CW. Osthole: A review on its bioactivities, pharmacological properties, and potential as alternative medicine. *Evid base Compl Alternative Med : eCAM*. 2015;2015:919616.
 30. Fan H, Gao Z, Ji K, et al. The in vitro and in vivo anti-inflammatory effect of osthole, the major natural coumarin from *Cnidium monnieri* (L.) Cuss, via the blocking of the activation of the NF- κ B and MAPK/p38 pathways. *Phytomedicine : International Journal of Phytotherapy and Phytopharmacology*. 2019;58(5):152864.
 31. Yun Y, Feng R, Ziyin T, Song W, Cheng B, Feng Z. Osthole synergizes with HER2 inhibitor, trastuzumab in HER2-overexpressed N87 gastric cancer by inducing apoptosis and inhibition of AKT-MAPK pathway. *Front Pharmacol* 2018;27(11):9-1392.
 32. Sun W, Cai Y, Zhang X-x., Chen H, Lin Y-d., Li H. Osthole pretreatment alleviates TNBS-induced colitis in mice via both cAMP/PKA-dependent and independent pathways. *Acta Pharmacol Sin*. 2017;38(8):1120-1128.
 33. Zhong-Rong Z, Wing NL, Gang L, et al. Osthole enhances osteogenesis in osteoblasts by elevating transcription factor osterix via cAMP/CREB signaling in vitro and in vivo. *Nutrients*. 2017;9(6):588.
 34. Sheng W, Yan X, YanWu H, et al. Airway relaxation mechanisms and structural basis of osthole for improving lung function in asthma. *Sci Signal*, 2020 ,24;13(659):eaax0273.

35. Arnaud M, Marie-Odile F, Nathalie D, Pereira B, Haas J, Lambert G. The comparative cytotoxic effects of different local anesthetics on a human neuroblastoma cell line. *Anesth Analg* 2015;120(3):589-596.
36. Nikhil KT, Srinath K, Ganesh SA. Channeling of cAMP in PDE-PKA complexes promotes signal adaptation. *Biophys J*. 2017; 112(12):2552-2566.
37. Hollmann MW, Wieczorek KS, Berger A, Durieux ME. Local anesthetic inhibition of G protein-coupled receptor signaling by interference with *gaq* protein function. *Mol Pharmacol*. 2001; 59(2):294-301.
38. Tamm I, Wang Y, Sausville E, Scudiero DA, Vigna N, Oltersdorf T, et al. IAP-family protein survivin inhibits caspase activity and apoptosis induced by Fas (CD95), Bax, caspases, and anticancer drugs. *Cancer Research*. 1998;58:5315-5320.
39. Tian FZ, Chang HS, Liu JX, Zheng J, Cheng D, Lu Y. Cynomorium songaricum extract alleviates memory impairment through increasing CREB/BDNF via suppression of p38MAPK/ERK pathway in ovariectomized rats. *Evid base Compl Alternative Med : eCAM*. 2019;2019: 20199689325.